

Network Analysis and Characterization of Vulnerability in Flood Control Infrastructure for System-level Risk Reduction

Hamed Farahmand^{1,*}, Shangjia Dong², Ali Mostafavi¹

¹ Zachry Department of Civil and Environmental Engineering, Texas A&M University, College Station, Texas, USA

² Department of Civil and Environmental Engineering, University of Delaware, Newark, DE 19716, United States

ABSTRACT

The number of catastrophic events such as extreme rainfalls and hurricanes has been growing. These events pose a major threat to the life safety and economic prosperity of urban regions. Flood control networks play a pivotal role in mitigating the risk associated with the stormwater generated by extreme rainfalls and hurricanes. The objective of this study is to propose a framework to examine the vulnerability in flood control infrastructure networks. This framework applies graph theory concepts and tools to define a vulnerability index for flood control network components (e.g., channels and rivers). The topological attributes of flood control networks are used to determine the vulnerability index based on structural attributes of flood control networks. First, a flood control network is modeled as a directed graph and storage facilities are incorporated into the network. Second, co-location exposure, upstream channel susceptibility, and discharge redundancy are characterized as important vulnerability attributes of a channel in flood control network. Then, these three characteristics are formulized based on the topological attributes of the network and characteristics of channels. The vulnerability index is then determined based on the three vulnerability characteristics. The proposed vulnerability index can be used to evaluate the impact of different risk reduction policies on flood control network vulnerability and determine the optimal mitigation strategies aiming at flood risk reduction, such as widening vulnerable channels, placement of storage facilities in the network or increasing the redundancy of the network. The framework is implemented on two watersheds in Harris County (Texas, USA) and the results' implications for decision-making in infrastructure management and hazard mitigation planning are discussed. The results highlight the capability of the proposed graph-based framework to inform flood risk reduction through evaluation of the vulnerability of infrastructure networks.

1. INTRODUCTION

Floods have caused a significant proportion of disaster-related economic and human losses [1] and pose a significant risk to urban infrastructure and community well-being in flood-prone regions [2,3]. It is projected that flood risk is intensified due to climate change-induced extreme weather events in the future [4–8]. In addition, rapid urbanization exacerbates flood risk by increasing the proportion of impermeable surfaces, which leads to higher peak and volume of runoff following an extreme rainfall [9–11]. Flood control infrastructure networks play a pivotal function in coping with flood risk in urban areas [12]. Hence, proper functioning of flood control networks can substantially reduce flood risk and impacts [13]. Flood control infrastructure includes different components such as dams and levees, reservoirs and basins, pumps and flood gates, and channel network. Flood control networks also include rivers, bayous, and ditches (all referred to as channels in this paper) whose function is draining stormwater runoff. The standard way of assessing the urban flood risk is using Hydraulic and Hydrologic models (H&H models) [14,15]. These models enable estimating the volume of runoff generated by different scenario rainfalls (such as 100-year and 500-year floods) and simulating the flood inundation in nearby neighborhoods [16,17]. However, H&H models have two major limitations in terms of informing about the vulnerability

44 of flood control networks. First, components of a flood control network have different levels of
45 vulnerability to disruption during a flooding event. To account for interdependencies in flood control
46 infrastructure, prioritization of flood risk reduction investments would require analysis of the topology of
47 flood control networks to identify the most vulnerable components. Second, hydrodynamic models allow
48 the representation of the flooded depth and the extent of the flooding areas. However, the translation of
49 such outputs for flood control infrastructure vulnerability assessment is rather limited. For example, the
50 spatio-topological configuration of the channel network as a system property can significantly affect flood
51 control performance. The existing H&H models, however, provide limited insights in performing system-
52 level flood control network vulnerability assessment and identifying the vulnerable infrastructure
53 components for prioritization of risk reduction investments. To address this gap, this paper proposes a
54 new graph-based methodology for vulnerability assessment of flood control networks. Through the use of
55 the graph-based methodology, a channel vulnerability index is defined as a combination of three
56 influencing characteristics: (1) co-location exposure, (2) upstream channel susceptibility, and (3)
57 discharge redundancy. Each attribute is determined using graph-based network measures. Accordingly,
58 the output of the proposed methodology identifies vulnerable channels for flood control infrastructure
59 enhancement to inform hazard mitigation and resilience management plans for flood risk reduction
60 prioritization.

61 The remainder of the paper is organized as follows. Section 2 provides a literature review on related flood
62 control network vulnerability analysis. Section 3 introduces the conceptualization of flood control
63 network vulnerability and describes the modeling approach for assessment of the vulnerability of
64 channels using graph theory. Section 4 illustrates the application of the proposed framework in two
65 watersheds located in Harris County (Texas, USA) and discusses the implications of the results for
66 policy-making in flood risk reduction. Section 5 summarizes the conclusions and contribution of the
67 study and discusses the limitations and future research directions.

68 **2. LITERATURE REVIEW**

69 Flood risk reduction strategies are categorized into four main groups including *resistance*, *avoidance*,
70 *acceptance*, and *awareness* strategies [18]. Conventionally, urban areas rely on *resistance* strategies in
71 which protective structures such as levees and dams are built to limit the inundation of downstream
72 regions. However, recent trends show that solely relying on *resistance* strategies is not effective for flood
73 risk mitigation [19]. It is generally argued that using a diverse set of strategies increases the redundancy
74 of the flood mitigation portfolios and leads to optimal risk reduction [20]. In this regard, researchers and
75 practitioners advocate the effectiveness of *avoidance* strategies in which the objective is to remove
76 development or steer it away from the most vulnerable areas and *acceptance* strategies, which allow
77 flooding in specific areas or under certain conditions to protect the other areas and provide a relief valve
78 when the volume of stormwater runoff is extensive [18]. Awareness strategies also focus on enhancing
79 the knowledge among citizens and decision-makers using tools such as social media outlets, education
80 and training programs, and workshops.

81 Flood control infrastructure networks play a pivotal role in devising and implementing *avoidance* and
82 *acceptance* strategies for flood risk reduction. In flood control networks, improving the performance of
83 the channel network by increasing the discharge capacity of channels is a standard *avoidance* strategy for
84 flood risk reduction [21]. Moreover, flood *acceptance* is often achieved through the construction of
85 storage facilities or dedicating open spaces for stormwater retention [22]. Therefore, proper management
86 of flood control networks can be achieved by focusing on both performance improvement of channel
87 network and development and maintenance of storage facilities that absorb the excessive stormwater,
88 which consequently reduces flood risks at the urban scale.

89 Performance of flood control networks is a function of the characteristics of different infrastructure
90 components such as reservoirs, dams, channels, and floodgates [23,24], as well as interdependencies
91 between the functionality of these different components [25–28]. Hence, vulnerability assessment of flood
92 control networks would require identifying the components that need to be prioritized to enhance the
93 performance of the network from a system perspective. For example, prioritizing channels for
94 enhancement or constructing new storage facilities should not be done based on the impact of the
95 enhancement project on the component itself, it should rather consider the changes of vulnerability in
96 other interdependent components of the system. The standard flood risk assessment is often conducted
97 using H&H models [16,29]. In these models, flow rates are estimated based on employing rainfall-runoff
98 and streamflow projecting models [15,30], as well as soil properties and topological structure of the flood
99 control network [31]. However, H&H models provide limited insights from an infrastructure risk
100 management and vulnerability assessment perspective. First, H&H models do not capture the
101 interdependencies in the flood control network [26]. Interdependence is a system-level phenomenon in
102 which the extent to which a component is vulnerable due to the potential negative impacts of other
103 interconnected components is characterized. Second, flood control networks have complex network
104 configurations in which the network attributes such as topology of the network is a determinant of the
105 system vulnerability [32,33]. Hence, network attributes of flood control infrastructure should be
106 considered in the assessment of vulnerability. Third, although H&H models can identify the high flood
107 risk regions, the resultant flood risk maps provide limited insights for infrastructure vulnerability
108 reduction. These flood maps often cannot inform the infrastructure network vulnerability reduction
109 decisions and help to devise proper strategies to reduce vulnerability from a system perspective.
110 Infrastructure network vulnerability reduction requires identification of the most susceptible channel
111 components and also ones that contribute to the vulnerability of the system as a whole [34]. Thus, there is
112 a need for system-level vulnerability assessment in the flood control network [26] to complement
113 standard H&H models for infrastructure prioritization towards flood risk reduction at the urban scale.

114 Modeling infrastructure network as a graph where individual infrastructure components are represented as
115 links or nodes has been shown as a powerful tool to analyze system attributes and interdependencies
116 affecting vulnerability [35]. Network analysis has been successfully applied to analyze vulnerability in
117 various infrastructures such as water, wastewater, road, and drainage networks [36–39]. A limited number
118 of studies have employed network analysis to examine flood control networks. For example, in the
119 context of artificial drainage networks, using network properties such as between-centrality, network
120 analysis has been used to identify sub-networks that can be independently managed [40]. In another
121 example, the application of network analysis has been shown for finding the optimal location of sensors
122 that are used to manage and control hydrologic infrastructures located on a flood control network. In this
123 regard, network properties are used to find the combination of sensors with maximum network coverage
124 [41]. Network theory and optimization would also help to select the location and size of retention basins
125 in a watershed, which results in the most cost-effective basin configuration that is also capable of
126 controlling flood optimally [42]. For pump operation management in retention basins and evaluating the
127 effect of capacity expansion on the resilience of the drainage network, the analysis of network topology
128 has been shown to be informative [43].

129 In another stream of research, several studies have focused on the application of network analysis for
130 assessment of vulnerability in the natural and artificial waterway systems. For example, network analysis
131 has been used for vulnerability assessment of deltaic systems [32], where different topological attributes
132 of the network have been employed to measure the complex and dynamic characteristics of delta
133 networks such as structural overlapping and entropy-based complexity [44]. Also, based on the analysis
134 of topological attributes in a network of channels, Ogie et al. [45] developed a methodology to quantify

135 the vulnerability of hydrological infrastructures such as pump stations and floodgates that are located in a
136 network of waterways [45,46]. Probabilistic network models such as Bayesian network analysis has also
137 been applied for the flood vulnerability assessment. In the methodology developed by Wu et al. [47], a
138 Bayesian network analysis approach was used to model temporal flow rates [47].

139 The review of the literature shows that network analysis can provide valuable insights for the assessment
140 of vulnerability in interconnected infrastructure that consists of a network of components (such as
141 channels and waterways). Despite the growing use of network analysis for examining infrastructure
142 systems and their interdependencies, vulnerability, and resilience, the existing literature lacks a graph-
143 based methodology and relevant measures for analyzing vulnerability in flood control networks to inform
144 infrastructure prioritization for urban-scale flood risk reduction. Due to the specific characteristics of
145 flood control networks (e.g., the need for consideration of flow and relationship between upstream and
146 downstream components), the existing graph-based methodologies (mainly based on percolation theory)
147 cannot be used for vulnerability assessment of flood control infrastructure. Hence, there is a need for a
148 graph-based methodology that can capture the characteristics of flood control infrastructure and help to
149 identify the components contributing to the vulnerability of the systems. To address this methodological
150 gap, this paper presents a new graph-based methodology to assess flood control network vulnerability. In
151 the proposed methodology, the vulnerability of channels in flood control networks is characterized based
152 on the susceptibility and exposure levels from the upstream channels and upstream storage facilities, as
153 well as the redundancy of the channel to discharge the stormwater runoff. Three network-based measures
154 are devised and examined to capture and represent the vulnerability of each channel in the network. The
155 resulting vulnerability index can be used for characterizing the spatial distribution of highly vulnerable
156 channels to inform flood risk reduction and infrastructure improvement programs. Besides, the results of
157 the proposed methodology would identify regions that are hotspots of vulnerability and could be a
158 candidate for the construction of storage facilities in immediate downstream based on consideration of
159 land availability [41]. Accordingly, the proposed graph-based methodology and measures can
160 complement the existing H&H models for assessment of the risk of flooding in urban areas.

161 **3. METHODOLOGY**

162 **3.1. Vulnerability in Flood Control Networks**

163 Different definitions and measures have been proposed for assessing vulnerability in infrastructure
164 systems [48–51]. According to Balica et al. [52], in case of flooding, the vulnerability of the system is the
165 encapsulation of its susceptibility to hazard disruption along with its capability to cope with, recover,
166 and/or adapt to the hazard. Vulnerability of a system component, in this definition, should capture three
167 essential attributes: (1) *exposure*: the extent to which a component is exposed to hazard (such as intense
168 flow rate); (2) *susceptibility*: the extent to which a component is susceptible to failure, disruption, or other
169 predefined adverse condition (such as overflow); and (3) *redundancy*: to what extent a component has
170 buffer (such as local retention) to avoid failure.

171 In case of flood control network vulnerability assessment, the inherent characteristics of each channel
172 (component), as well as the spatio-topological properties of the network need to be examined. This study
173 considers the discharge capacity as the most significant inherent characteristic of channels in the
174 assessment of vulnerability. The analysis of vulnerability also considers three attributes of channels that
175 are derived from the position of the channel in the network topology. A combination of these three
176 attributes along with the discharge capacity can be used for characterizing the vulnerability of a channel.
177 In this context, the exposure and susceptibility of channels are attributed to the volume of stormwater in

178 the upstream of the channel. However, there are three inherently different sources of hazard-causing
179 exposure and susceptibility for a channel as explained below.

180 **Susceptibility:** Stormwater runoff in the channels in the upstream of a channel pose a risk to the
181 downstream channel. The stormwater runoff from the upstream can potentially cause an overflow in the
182 downstream channel and surrounding neighborhoods [32,44]. The greater the volume of stormwater in the
183 upstream channels, the greater the exposure to the flood risk in the channel. In addition, the higher
184 relative capacity of a downstream channel compared to channels in upstream means that the channel is
185 less susceptible to the increased flow in the upstream channels.

186 **Exposure:** Stormwater runoff stored in storage facilities (such as retention basins or reservoirs) in the
187 upstream of a channel exposes the channel to a significant surcharge of stormwater if the generated
188 stormwater runoff exceeds the capacity of the facility. In other words, the channel is also at risk of
189 overflow in case of an exceedance of stormwater runoff from the capacity of storage facilities in the
190 upstream. Hence, exposure is a function of proximity to the storage facility in the upstream and the risk of
191 overflow in the facility. The risk of overflow is also a function of the volume of stormwater that the
192 storage facility is designed to absorb (i.e., stormwater runoff in the upstream of the facility), as well as the
193 capacity of the storage facility to store stormwater runoff.

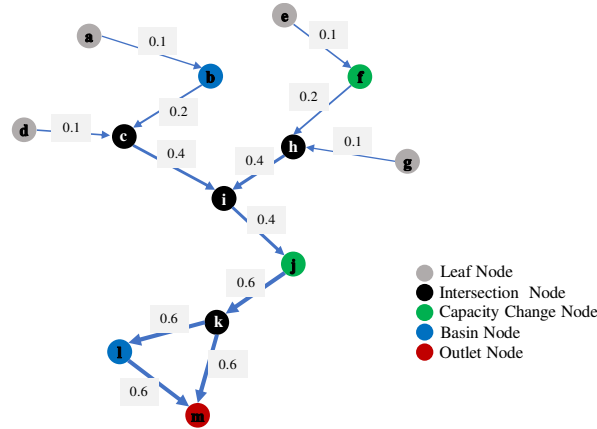
194 While exposure and susceptibility increase the vulnerability, there is another attribute (i.e., redundancy)
195 that reduces the vulnerability of a channel. Redundancy is a positive attribute of a component or a system
196 capturing the extent of buffer in case of a disruption. For the case of the flood control network,
197 redundancy is characterized as follows:

198 **Redundancy:** Redundancy refers to the ability of a channel to properly discharge the stormwater runoff
199 flow to the downstream [24]. The redundancy is a function of (1) the number of alternative paths that the
200 channel relies on to discharge the runoff and (2) the possibility of blockage in stormwater discharge (If a
201 channel is close to a sink node such as a storage facility or an outlet, the channel is subject to less flood
202 risk due to the blockage in the downstream channels). In other words, building a storage facility in the
203 downstream increases the redundancy of channels in the upstream by absorbing the risk of blockage in the
204 downstream channels.

205 **3.2. Modeling Flood Control Network using Graph Theory**

206 In modeling the flood control network as a directed graph, each elements of vulnerability can be
207 formulated based on the definitions provided in the previous section and utilizing channel characteristics
208 and network topology. A flood control network consists of a set of spatially connected channels that drain
209 stormwater runoff generated by extreme rainfalls to the outlet(s) (which are either naturally existed or
210 artificially built to prevent inundation and overflow in the neighborhoods). Considering each channel as
211 an edge, a flood control network can be modeled as a graph $G = (V, E)$, in which channels are the links
212 $E \subseteq \{e_{ij} | e_{ij} \in V^2\}$, and nodes $V = \{v_1, v_2, \dots, v_n\}$ are the joints connecting the channels or storage
213 facilities. In addition, there is generally no loop in gravity-based flood control systems. Hence, a flood
214 control network can be modeled as a Directed Acyclic Graph (DAG). Figure 1 shows a schematic
215 representation of the DAG model of a flood control network. In the DAG model, edges are the channels
216 and the discharge capacity of edges can be attributed to the weight of edges. For example, in Figure 1,
217 where channel weights are shown on the channels, the discharge capacity of channel bc (0.2) is twice
218 more than the discharge capacity of channel ab (0.1). Nodes in the DAG model of channel networks can
219 have different attributes. For example, nodes can represent transition points where channel capacities
220 changes, channel intersections, basins, or outlets. In the DAG model of the flood control network, edges

221 have different attributes such as length and flow capacity that can be used to characterize vulnerability.
 222 Flow capacity is the maximum rate of discharge that a channel can provide.



223
 224 **Figure 1. Modeling a network of channels as a Directed Acyclic Graph (DAG) consist of channels with different capacities**
 225 **and different types of nodes**

226 For calculation of vulnerability attributes, we applied topological ordering in the DAG model of channels.
 227 For graph $G = (V, E)$, an ordered list of nodes $\Omega = \{v_1, v_2, \dots, v_n\}$ is called a topological ordering if for
 228 all edges $v_i v_j \in \Omega$, then $i < j$. Algorithm 1 can be used to perform topological ordering in a DAG and
 229 generate a sorted listed of nodes in a graph [53]. A sorted list of a directed graph can ease determining the
 230 set of channels and storage facilities in the upstream and downstream of a channel and facilitates the
 231 calculation of attributes that are defined to characterize vulnerability in flood control networks in this
 232 study. In the following sub-section, we formulate the vulnerability attributes described in Section 3.1, and
 233 then, combine these three attributes to devise a channel vulnerability index.

Algorithm 1. Topological Sorting of Graph G

Procedure Topological Sort
Input: $G(V, E)$ # G is a directed graph, and d is the ordered set of node indexes of G

- 1 set all nodes to be unindexed
- 2 **for** $i = 1, \dots, n$
- 3 select any unindexed node v that all its parents are unindexed
- 4 $d(v) \leftarrow i$
- 5 Mark v
- 6 **Return:** (d)

234
 235 **3.3. Formulation of Channel Vulnerability in Flood Control Network**

236 **3.3.1. Co-location Exposure**
 237 Overflow risk exposure in co-located storage facilities in the upstream can contribute to a channel's
 238 vulnerability [54]. In this framework, we consider the overflow risk of a storage facility based on the ratio
 239 of the stormwater volume in its upstream to its storage capacity as follows:

240
$$\Gamma_b = \frac{Exposure_b}{Cap_b} \quad (1)$$

241 Where Γ_b represents overflow risk of a storage facility b , $Exposure_b$ is the volume of stormwater that
 242 can be stored in the channels in the upstream of facility b , and Cap_b is the capacity of facility b . The
 243 lower the ratio, the more capable the facility to absorb the upstream stormwater and prevent overflow in
 244 the downstream channels. From a flood control perspective, storage facilities such as retention basins can

245 be designed and constructed to reduce the risk of overflow in the downstream by collecting the runoff
 246 generated in the upstream. In case the runoff inflow exceeds the design capacity of the facility, the
 247 downstream channels are exposed to risk of excessive flow that could cause overflow. Therefore, to
 248 characterize the exposure for a channel, we need to know (1) the storage facilities in its upstream and the
 249 distance between them, which impacts the exposure risk, and (2) the exposure risk of the facilities that
 250 contributes to the vulnerability of the channel. Considering these two factors, we designed Algorithm 2
 251 for quantifying the co-location exposure risk of each channel.

252 Algorithm 2 presents the procedure for calculating Co-Location Exposure (CLE) in each channel. The
 253 procedure can be divided into three steps. First, the overflow exposure for each storage facility is
 254 calculated (sub-algorithm 2.1) by summing up the storage capacity of all the upstream channels, which
 255 for each channel is the volume of stormwater that can be stored in the channel. For example, in the
 256 channel network in Figure 1, exposure for storage facility b is equal to the storage capacity of channel ab
 257 that equals the length of channel ab multiplied by the area of the channel cross-section. For storage
 258 facility l , all the channels in its upstream contribute to the exposure of the facility, which include all
 259 channels in the network except channel ab and channels km and lm . Then, for each channel, the storage
 260 facilities located in the upstream of the channel are identified (sub-algorithm 2.2). Finally, the CLE of a
 261 channel is calculated given the overflow exposure of its upstream storage facilities and the distance
 262 between the channel and the storage facility ($dis_{i,b}$), by summing over all upstream facilities (sub-
 263 algorithm 2.3). for example, in Figure 1, both facilities b and l contribute to the CLE of channel lm , while
 264 only facility b is considered for calculation of C=the CLE of channel ci , and there is no facility
 265 contributing to the CLE of channels in the upstream of node h . It should be noted that for the calculation
 266 of overflow risk for a facility, only the channels that are located between the facility and facilities in the
 267 upstream are calculated. The assumption is that each storage facility absorbs the stormwater runoff for all
 268 channels in its upstream, and therefore, no risk exposure would be transferred to the other storage
 269 facilities in downstream. However, it should be noted that this assumption does not consider cases that
 270 multiple storage facilities may fail concurrently and overflow in the upstream facility can impact the
 271 facility in downstream. Integration of concurrent failure risk should be addressed in the future research.

Algorithm 2. CLE Calculation for Graph χ

Procedure: CLE Calculation

Input: $\chi(V, E, l, A), B \subset V, d$ # B includes storage facilities, and d is topological-sorted of χ , l includes
 lengths of channels, and A includes areas of cross-section of channels

sub-algorithm 2.1: calculating exposure of each facility

1 **for** b in d

2 **if** b is in B

3 $Upstream(b) = []$ #Upstream includes all channels in the upstream of channel b

4 $Upstream(b) \leftarrow$ all edges in upstream $\subset E$

5 $Exposure(b) \leftarrow$ sum over $A \times l$ for edges in $Upstream(b)$

6 remove $Upstream(b)$ from E

sub-algorithm 2.2: assign storage facilities of each channel

7 **for** i in E

8 $SF(i) \leftarrow$ storage facilities in upstream of i # SF contains storage facilities in upstream of the channel

sub-algorithm 2.3: calculate CLE for each channel

9 **for** i in E

10 **for** b in $SF(i)$

11 $dis_{i,b} \leftarrow$ node distance between i and b # $dis_{i,b}$ is the topological distance between channel and the
 storage facility

12 $CLE(i) += \frac{1}{dis_{i,b}} \times (1 + \frac{Exposure(b)}{Cap(b)})$

13 **Return:** χ

272

3.3.2. Upstream Channel Susceptibility

Flow dynamics of flow transport is one of the factors greatly influence the vulnerability of the channels in flood control networks. H&H models quantify flow transport dynamics using the differential equations as well as hydrology and surface characteristic inputs. In this study, we adopted the approach developed by Tejedor et al. (2015) [32] to consider the transport dynamics in graph-based analysis of river and channel networks. To do so, we developed Upstream Channel Susceptibility (UCS) index that examines the extent to which a change in flow of upstream channels can impact the flow of a channel by aggregating impacts that the flow from all its upstream channels inflict on the channel of interest. Algorithm 3 shows the calculation procedure. To calculate the UCS value for each channel, first, a fixed percentage of increase in the flow of the channel is considered (ρ). The influence of upstream channel u on the susceptibility of channel i is denoted by η_{iu}^ρ , which shows the ratio of increase in flow of channel u that leads to increase in flow of channel i in the downstream of u by ratio ρ . In this calculation, it is assumed that the flow of channel i is influenced by channels that are in the upstream of channel i but not in the upstream of any storage facility that channel i is exposed to. In fact, the influence of channels in the upstream of any storage facility that channel i is exposed to considered to be absorbed by the facility and the risk of overflow is reflected in the calculation of CLE. For example, in Figure 1, the flow in the channel ci is influenced by the changes in the flow of channels bc and dc , and the influence of channel ab is considered in the CLE of the channel that considers the overflow risk of facility b .

A high UCS value means that a channel is susceptibility to the increase in flow of channels in the upstream. A high UCS value can be due to: (1) lower capacity of a channel compared to the channels in the upstream and (2) the channel being linked to a large number of channels in the upstream. To reduce the UCS, additional storage facilities can be added in the upstream of the channel to reduce the number of channels in the upstream whose flows lead to the downstream channel. Increasing the downstream channel capacity can also reduce its susceptibility. Thus, the UCS measure also captures the extent to which an increase of discharge capacity in a channel leads to an increase in the vulnerability of other channels in the downstream. Accordingly, the UCS measure informs infrastructure enhancement decisions considering the system-level impacts of the decision rather than focusing on the regional consequence of an enhancement project.

Algorithm 3. UCS Calculation for Graph χ

Procedure: UCS Calculation

Input: $\chi(V, E, l, A), B \subset V, d, \rho$ # B includes storage facilities, and d is topological-sorted of χ , l includes lengths of channels, and A includes areas of cross-section of channels

```

1  for  $e$  in  $E$ 
2     $SF(e) \leftarrow$  storage facilities in upstream of  $FN(e)$  #  $FN(e)$  is the start node of the channel  $e$ 
3     $\psi \leftarrow$  Reversed( $d$ ) #reversed of the topological ordered list of nodes in the channel network
4     $Upstream(e) \leftarrow$  edge in  $\psi$  that is in  $Upstream FN(e)$  and not in  $\cup_{j \in SF(e)}(Upstream(j))$ 
5    for  $u$  in  $Upstream(e)$ 
6       $increased(u) = (1 + \rho) \times Capacity(e)$ 
7       $reduceCap(u) = \min(\text{sum}(Capacity(adjacents(u)), 0.9 \times Capacity(neighbor(u))))$ 
8       $UCS(e) += \frac{(increased(u) - reduceCap(u))}{increased(u)}$ 
9  Return:  $\chi$ 

```

3.3.3. Discharge Redundancy

Discharge Redundancy (DR) of a channel depends on the number of sink nodes that the channel can drain to (i.e., outlets and basins in the downstream). DR captures the redundancy of the channel to discharge stormwater runoff in case of a disruption in the downstream. Any disruption in the downstream of a channel influences the stormwater flow in the channel and can cause runoff propagation into the

307 neighborhood. For example, blockage of channels in the downstream due to sediment or debris
 308 accumulation could lead to overflow in upstream channels. Two factors could impact the redundancy of a
 309 channel. First, the higher number of paths to sink nodes increases the discharge redundancy since, in case
 310 of blockage in a path, an alternative path can discharge the stormwater flows downstream. Second,
 311 discharge redundancy is influenced by the distance between a channel and sink nodes. In this regard, any
 312 downstream blockage could cause runoff backpropagation. The risk of blockage is associated with the
 313 length and size of the channels that connect the channel to the sink node. A longer and larger channel
 314 poses higher risk of blockage [4]. DL is calculated by assigning weights to different paths between
 315 channels and sink nodes, where path's weights are functions of the distance between the channel and the
 316 sink node. Thus, discharge redundancy is calculated by assigning weights to different paths between
 317 channels and sink nodes, where a path's weights is a function of the distance between the channel and the
 318 sink node. The summation of the weighed paths, then, determines the discharge redundancy of a channel.

Algorithm 4. DR Calculation

Procedure: DR Calculation

Input: $\chi(V, E, l, A), B \subset V$, # B includes storage facilities, and d is topological-sorted of χ , l includes
 lengths of channels, and A includes areas of cross-section of channels
 1 Sink $\leftarrow \chi.outlets, B$ #Sink includes the outlet of the channel network (node with outdegree equal
 zero)
 2 **for** e in E
 3 **for** s in Sink
 4 **If** haspath($\chi, TN(e), s$) # $TN(e)$ is the end node of the channel e
 5 $d = |path(TN(e), s)|$ # d is the topological length of path between the channel and the outlet
 6 $DR(e) += w(d)$ # $w(d)$ is the weighted value of d
 7 **Return:** χ

319

3.3.4. Channel Vulnerability Index

320

321 The vulnerability of a channel is a function of CLE, UCS, and DR. CLE and UCS would increase the
 322 channel vulnerability while DR would reduce its vulnerability. Accordingly, we characterize the channel
 323 vulnerability index ζ using Equation (2) [55].

324

$$\zeta_e = f(CLE_e, UCS_e, DR_e) = \frac{CLE_e \times UCS_e}{DR_e} \quad (2)$$

325

326 The channel vulnerability index calculated using Equation (2) evaluates the vulnerability of channels
 327 from a system-level perspective considering the structural and topological characteristics of the channel
 328 network, as well as characteristics of each channel that impact its ability to discharge stormwater without
 329 an occurrence of overflow in the neighborhood of the channel. It should be noted that the proposed
 330 approach for vulnerability assessment is based on characteristics of physical infrastructure and does not
 331 consider rainfall scenarios. In fact, the vulnerability assessment framework presented here aims at
 332 identifying the channels and areas in the network that need to be prioritized for channel improvement or
 333 basin construction projects that reduces the risk of inundation in the area regardless of the extent of
 hazards such as rainfall duration and peak value, as well as distribution of rainfall.

334

4. FLOOD CONTROL NETWORK VULNERABILITY IN HARRIS COUNTY

335

336 The application of the proposed methodology and measures was demonstrated in two major watersheds in
 337 Harris County, Texas (USA). Harris County is the third-largest county in the United States and has more than
 338 4,023 km of channels in its flood control network. It comprises 22 watersheds, all of which drains into
 339 Galveston Bay. The flood control system in Harris County performs well under normal rainfall. Extreme

340 weather events such as hurricane Harvey, however, can pose a great risk to the county and cause urban
 341 flooding. Using the proposed graph-based method and measures, we examined the flood control network
 342 vulnerability in two major watersheds in Harris County: Brays bayou and Greens bayou watersheds. Both of
 343 these watersheds experienced extensive floods over the past decade including Tax Day Flood (2016),
 344 Memorial Day Flood (2016), and Hurricane Harvey (2017). Table 1 shows the characteristics of the
 345 studied watersheds.

346 *Table 1. Characteristics of Brays bayou and Greens bayou Watersheds* [56]

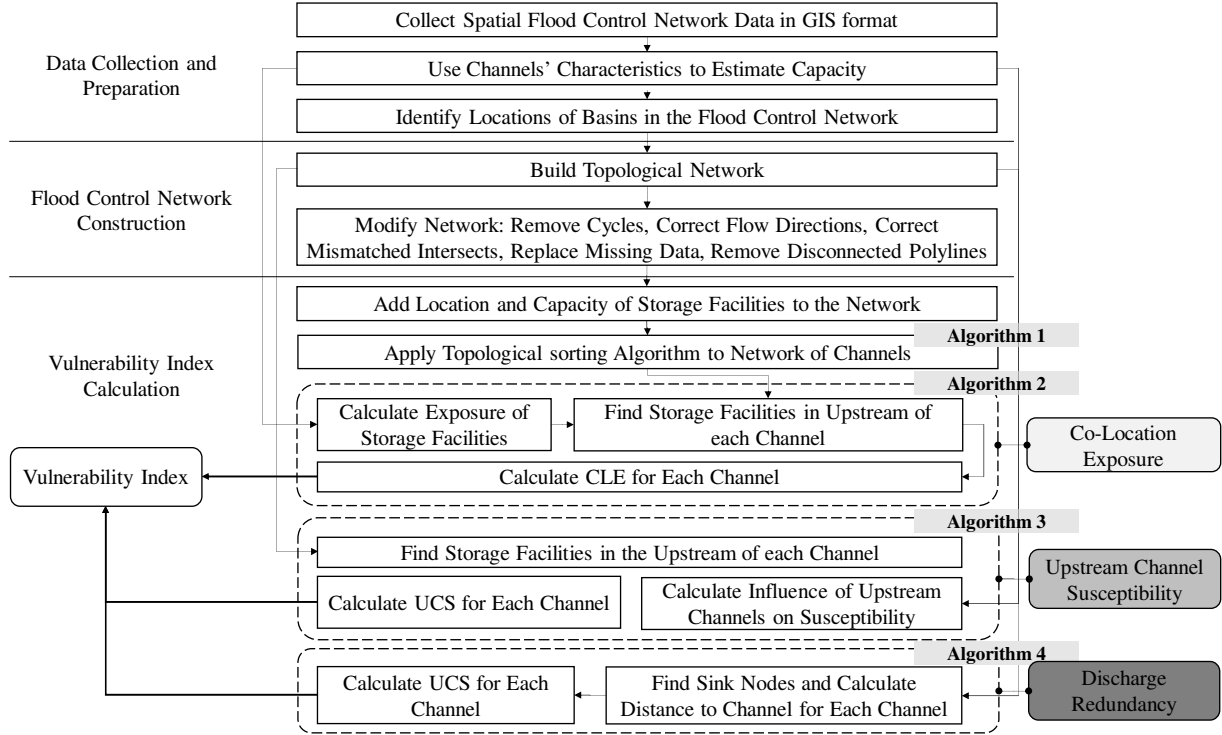
Characteristic	Watershed	
	Brays bayou	Greens bayou
Drainage Area (sq. Miles)	127	212
Open Streams (Miles)	12	308
Population (2010 U.S. Census)	717,198	528,720
Primary Streams	Brays bayou Keegans bayou Willow Waterhole bayou	Garners bayou Greens bayou Halls bayou Reinhardt bayou

347

348 **4.1. Analysis Procedure**

349 To demonstrate the application of the graph-based methodology and measures in the two watersheds in
 350 Harris County, we use the procedure presented in Figure 2. First, we collected and processed the GIS data
 351 of the flood control networks in the watersheds. Flow capacity of channels as well as location and storage
 352 capacity of the storage facilities were estimated. Then, the network of channels was constructed using the
 353 GIS data of the network. The network was modified in order to remove errors such as incorrect flow
 354 directions, disconnected polylines, and mismatched intersections. Storage facilities were incorporated in
 355 the network model, and then, different attributes of vulnerability as well as the vulnerability index were
 356 calculated for each channel using the algorithms elaborated in the previous section. Finally, the results
 357 were mapped and examined in order to assess the vulnerability of the flood control network in the study
 358 area from a system-level perspective, and the implications of results for infrastructure vulnerability
 359 reduction were identified.

360



361

362

Figure 2. Overview of the Proposed Framework

363 **4.2. Data Collection and Network Modeling**

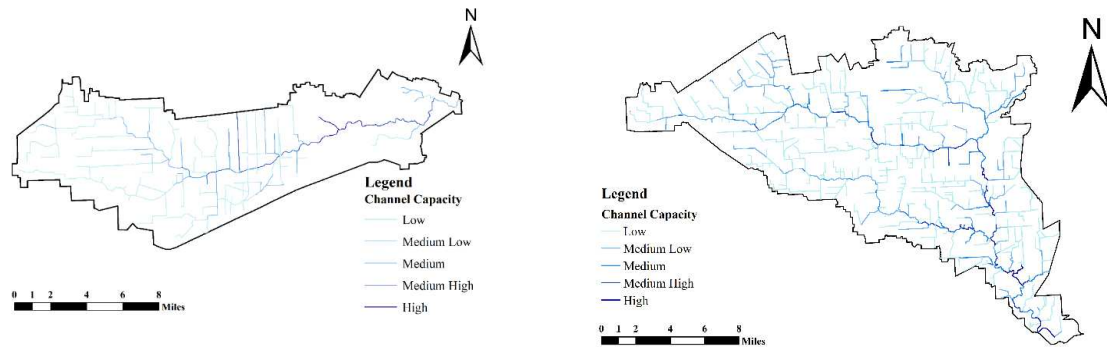
364 The capacities of channels were estimated using the Manning equation (Equation (3)):

365
$$(Q_c)_{ij} = \frac{\alpha}{n_{ij}} \times (A_{ij})^{\frac{2}{3}} \times (R_{ij})^{\frac{1}{2}} \times (S_{ij})^{\frac{1}{2}} \quad (3)$$

366 Where $(Q_c)_{ij}$ is the flow capacity of channel ij , α is a constant, n_{ij} is manning coefficient for channel ij ,
 367 A_{ij} is the area of cross-section of channel ij , R_{ij} is the hydraulic radius of channel ij , and S_{ij} is the slope
 368 of the channel ij . For the channels with missing data, the capacity of adjacent channels was used to
 369 estimate the discharge capacity. Figure 3 schematically shows the distribution of channel capacities in
 370 two watersheds.

371

372



(a) **Figure 3. Capacity of Channels in the Flood Control Network** (b)

373

374 Figure 4 shows the map of the flood control network and the storage facilities in the study area. Flood
 375 control network data of the two studied watersheds in Harris County is provided by Harris County Flood
 376 Control District (HCFCD) [56], including channel characteristics, the geographic location of each
 377 channel, as well as the connection of channels. In addition, the storage facility data were collected
 378 through organizational websites and reports. We mapped the information to its closest node in the
 379 network [56]. The storage capacity of the facilities was also gathered from the official documents
 380 (summarized in Table 2). For the missing data, the capacity was estimated based on the area of the
 381 facility. Based on abstracting the flood control network and modeling it as a DAG, there are 224 nodes
 382 and 223 edges in Brays bayou watershed and 692 nodes and 691 edges in Greens bayou watershed.

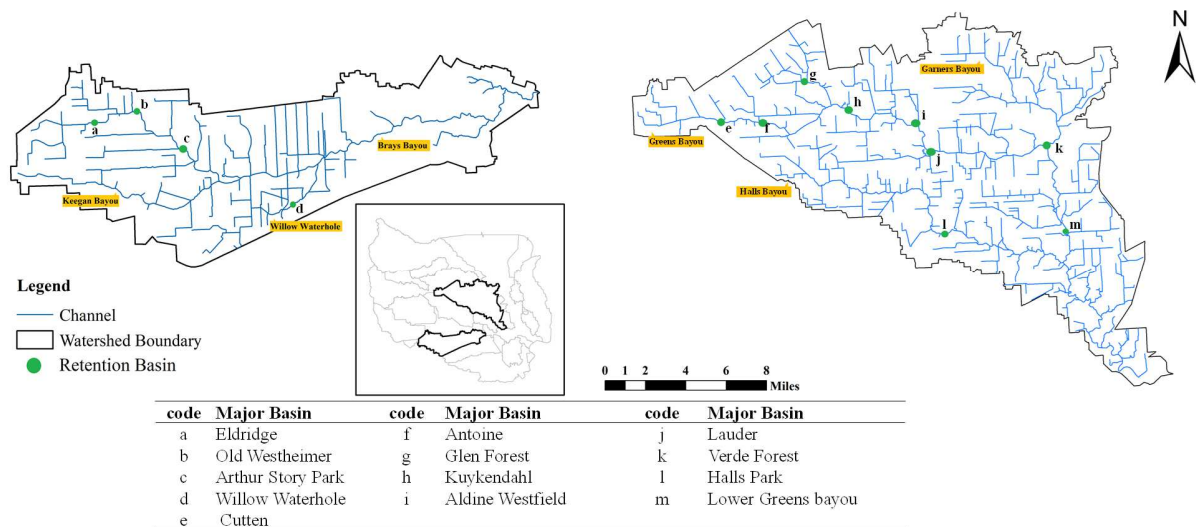
383

Table 2. Characteristics of Bains in Brays Bayou watershed

Major Retention Basin	Capacity ($gal \times 10^6$)
<i>Brays bayou watershed</i>	
Old Westheimer	200
Eldridge	1,500
Willow Waterhole	600
Arthur Story Park	1,100
<i>Greens bayou watershed</i>	
Kuykendahl	757.6
Glen Forest	291.3
Cutten	300*
Halls Park	231
Antoine	538
Lauder	391
Aldine Westfield	407.3
Verde Forest	1,360
Lower Greens bayou	765.4

384

*estimated (no data available)



385

386

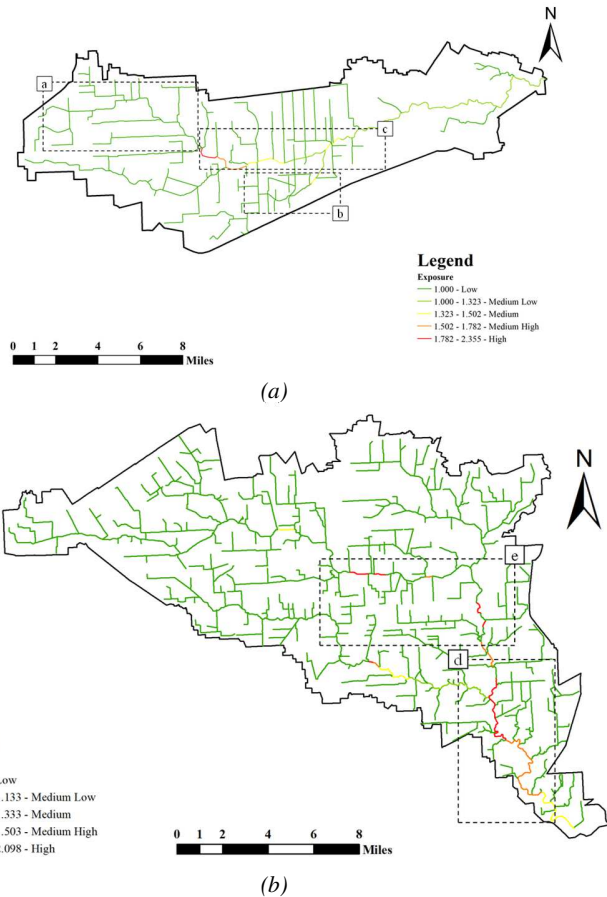
Figure 4. Study Area and Topology of Flood Control Network

387 4.3. Flood Control Network Vulnerability Assessment

388 In this section, the results related to implementing the proposed framework for vulnerability assessment
 389 of flood control network in the study area are presented. The three attributes of vulnerability are
 390 calculated for all channels in the study area, results are mapped, and discussed. Moreover, the
 391 implications of the results for decision-making in infrastructure vulnerability reduction are discussed.

392 4.3.1. Co-location Exposure Mapping

393 Figure 5 shows CLE for channels in Brays bayou and Greens bayou watersheds. In Brays bayou
 394 watershed, it can be seen that the channels that flow to the bayou have low CLE (box a). The result
 395 indicates that the storage facilities are located in this region are capable of absorbing the stormwater
 396 runoff in the upstream. In the Waterhole bayou, however, there are channels with medium CLE located in
 397 the downstream of the storage facility (box b). It indicates that the facility requires more capacity to
 398 absorb the upstream runoff in case of a flood. In addition, in the Central part of Brays bayou and in the
 399 downstream of the Aurthr Story Park basin (box c) the CLE is relatively high. Although the basin may be
 400 able to properly absorb the low-intensity rainfall, however, the high CLE shows that the downstream of
 401 the basin are vulnerable due to the overflow of the basin in case of extreme rainfalls. In the Greens bayou
 402 watershed, high CLE can be observed in the downstream, specifically, in the neighborhood of the Lower
 403 Green bayou basin (box d). The high value of CLE is due to the high overflow risk from the co-located
 404 basin. Also, CLE in the downstream of the basin located in Halls bayou is high, and consequently, the
 405 CLE for the channels in the downstream of the intersection of the Garners bayou and Halls bayou is
 406 impacted by the co-location effect between the two bayous (box e). This result shows an example of the
 407 impact of network topology on the vulnerability of channels.



408 **Figure 5. CLE Map for two watersheds' channels; (a) Brays bayou and (b) Greens bayou**

408

409 **4.3.2. Upstream Channel Susceptibility Mapping**

410 In the next step, we calculated the upstream channel susceptibility (UCS). Figure 6 shows the UCS map
 411 of the study area. As shown in Figure 6 (a), the UCS in Brays bayou is significantly higher in the
 412 mainstream of Brays bayou (box a) compared to the other channels that flow into the mainstream. This
 413 result shows the extent to which the susceptibility of each channel is affected by its position in the
 414 network topology. In the case of Brays bayou, the construction of basins would be a proper policy to
 415 absorb the impact of upstream channels. However, the space limitation for the construction of large basins
 416 often leads to reliance on channel enhancement and widening. Such projects currently form a majority of
 417 flood risk reduction projects in Brays bayou watershed [57]. It is also worth noting that the presence of
 418 storage facilities, which are responsible for absorbing the influence of upstream channels' susceptibility
 419 leads to low UCS in the Northwest of the watershed (box b).

420 Figure 6 (b) shows the UCS map for the Greens bayou watershed. As opposed to Brays bayou, Greens
 421 bayou is formed by smaller sub-network of channels that converge in the downstream of the watershed.
 422 Therefore, the distribution of UCS is sparser throughout the watershed. However, the mainstream of
 423 Greens bayou and Halls bayou have channels with high UCS (box c). The topology of the sub-network,
 424 which has a similar structure as Brays bayou watershed and lack of any storage facility contributes to the
 425 high UCS in this mainstream. Also, the Northwest of the watershed (box d) has generally low UCS due to
 426 the presence of storage facilities that can control the increase of flow in the upstream channels.

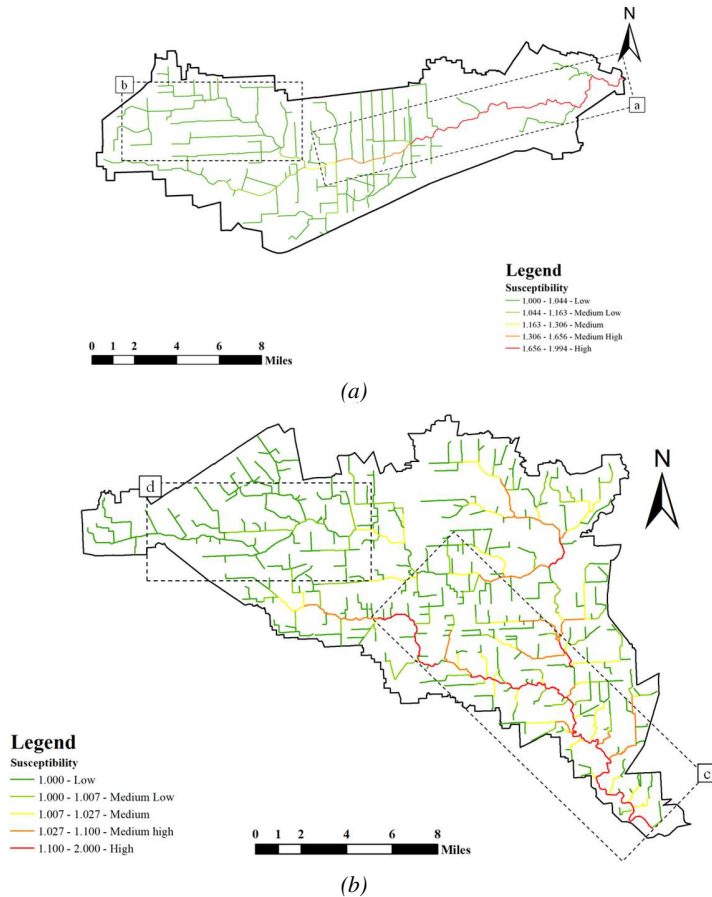


Figure 6. UCS Map for two watersheds' channels; (a) Brays bayou and (b) Greens bayou

427

4.3.3. Discharging Redundancy Calculation

428

429

430

431

432

433

434

435

436

437

Discharge redundancy was also calculated for channels in the network. Channels in the Northwest part of Brays bayou watershed have generally higher DR, however, channels in the upstream of the main branch of Brays bayou have generally less redundancy. This is due to the fact that these channels have high distance from the outlet and there is no alternative sink node in their downstream. In the Greens bayou watershed, considering the impact of storage facilities and the outlet, the DR for a majority of channels in Greens bayou is high, while in the contrary, channels in Halls bayou and Garners bayou have lower redundancy. Generally, the flood control network in Brays bayou and Greens bayou are tree-like; therefore, the number of different paths to sink nodes is one, which reduces the discharge redundancy of channels.

4.3.4. Flood Control Network Vulnerability Index

438

439

440

441

442

443

444

445

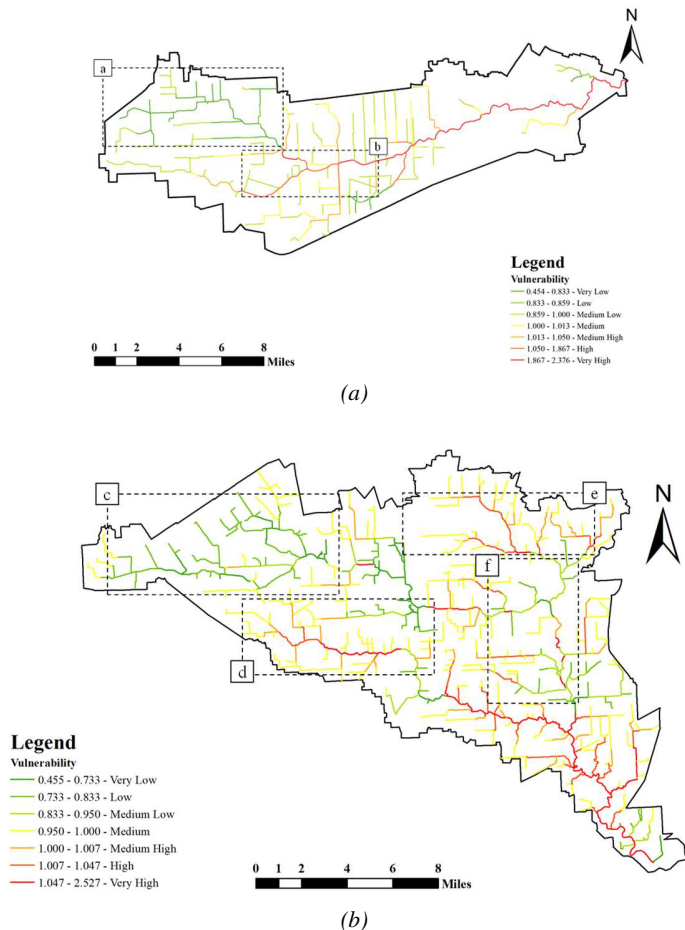
446

447

Combining the impacts of co-location exposure, upstream channel susceptibility, and discharge redundancy, the vulnerability index created in this study can represent the overall vulnerability of channels. Figure 7 shows the channel vulnerability index for Brays bayou and Greens bayou watersheds. The results show that in the Northwest of Brays bayou watershed (box a), the vulnerability index is low, which is due to the presence of well-distributed storage facilities with sufficient capacity to absorb the upstream stormwater runoff (providing discharge redundancy for the channels in the upstream). The channel sections in the mainstream of the Brays bayou are highly vulnerable. In the region close to the intersection of Keegan bayou and Brays bayou (box b), the main cause of the vulnerability is the high distance to sinks and the presence of a basin with high overflow risk in the vicinity. Although these

448 impacts are reduced in the downstream channels, the absence of any storage facility increases UCS. A
 449 common approach for vulnerability reduction in such cases would be enhancing channel flow capacity.
 450 However, any increase in the flow capacity of channels in the upstream would increase the susceptibility
 451 of channels in the downstream. In this case, upstream channels would be able to collect a high volume of
 452 stormwater runoff, however, the downstream would not be able to drain the excessive volume of runoff
 453 collected by the upstream channels, and therefore, overflow would be expected. Consequently, any
 454 enhancement project needs to consider the impact of network topology on the vulnerability in the network
 455 instead of focusing on increasing flow capacity in a specific region.

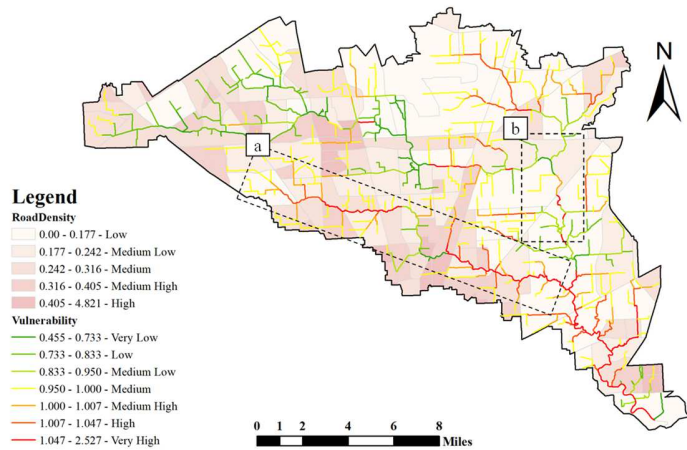
456 A similar pattern can be seen in the Greens Bayou watershed (Figure 7 (b)). The proper distribution of
 457 basins with sufficient storage capacity led to a low vulnerability in the Northwest of the watershed (box
 458 c). On the contrary, the lack of storage facilities as well as the configuration of channels in the Southwest
 459 part (box d) led to the formation of clusters of vulnerable channels. A similar situation is observed in the
 460 Northeast part of the Greens bayou watershed (box e). The presence of Lower Green bayou and Verde
 461 Forest basins that are capable of absorbing excessive runoff has reduced the vulnerability in the middle
 462 part of the Garners bayou (box f).



463 **Figure 7. Vulnerability for Flood Control Channels in (a) Brays bayou, and (b) Greens bayou**

464 **4.4. System-level Flood Risk Reduction Implications**

465 System vulnerability results from its intrinsic characteristics and the decisions made by managers and
466 operators. Proper vulnerability assessment should (1) help practitioners and decision makers to better
467 understand the causes and profile of vulnerability in the system and (2) enable evaluating the impacts of
468 different policies on the vulnerability reduction. The proposed framework achieves both criteria by
469 examining vulnerability from a system perspective. For example, we discussed the potential of enhancing
470 channels and construction of storage facilities as a structural solution for vulnerability reduction in the
471 flood control network. However, construction of storage facilities often requires availability of open land,
472 which might not be feasible in metropolitan areas due to limited spaces. Hence, prior to recommending
473 construction of retention basins, we may need to assess limitations for policy implementation. In this
474 paper, we used road density as an indicator of open space availability to assess the feasibility of storage
475 facilities in a watershed. The association between road density and urban expansion [5] proves that road
476 density is a proper structural indicator for land use transition, as a higher density of road network
477 indicates a lower open space availability [58]. To examine the feasibility of retention basin development
478 for reducing upstream susceptibility, we overlaid the vulnerability map of flood control network in
479 Greens bayou watershed with the road density map (aggregated in census tract level), measures in
480 Miles/Sq. Miles unit, as shown in Figure 8. It can be seen that, although the construction of a storage
481 facility can reduce the vulnerability of channels in the downstream of Halls bayou (box a), it is practically
482 infeasible due to the unavailability of open spaces. On the contrary, the channels located in the
483 downstream of the intersection of the Garners bayou and Greens bayou (box b) have low vulnerability,
484 which is due to the presence of storage facilities. The road density map shows that the construction of
485 these facilities was a feasible option in these areas. Similarly, in the Southwest of the watershed, the
486 construction of storage facilities may reduce the vulnerability of channels since the map shows that there
487 should be sufficient open spaces in the region.



488

489

Figure 8. Flood control network vulnerability vs. road density in Greens bayou

490 **5. CONCLUDING REMARKS**

491 This paper presents a graph-based methodology and measures for analyzing and characterizing
492 vulnerability in flood control infrastructure (e.g., channels and rivers). The proposed methodology departs
493 from the existing H&H models for analyzing urban-scale flood risk due to: (1) its focus on flood control
494 systems to inform infrastructure prioritization; (2) its capability to capture structural topology and
495 interdependencies among different channels in assessment of vulnerability; (3) its characterization of
496 vulnerability based on three fundamental attributes: Co-Location Exposure (CLE), Upstream Channel

497 Susceptibility (UCS), and Discharge Redundancy (DR); (4) its ability to examine system-level effects of
498 risk reduction measures; and (5) its ability to evaluate channel vulnerability without the need for
499 extensive data and computational resources and efforts (as usually required in H&H modeling).

500 The application of the proposed methodology and measures in two watersheds in Harris County shows
501 the capability of the proposed vulnerability characterization framework and index in identifying the
502 vulnerable channel components. The results of the case study show that, other than the properties of
503 channels and network structure, storage capacity can significantly impact the spatial patterns of
504 vulnerability in the flood control network. For example, the Northwestern region of Greens bayou
505 watershed presents lower vulnerability due to the presence of distributed storage facilities. In the
506 downstream of the Garners bayou, the abundance of open spaces for storage of runoff contributes to the
507 low vulnerability of channels in this region. In densely urbanized areas such as the downstream of Halls
508 bayou where the construction of storage facilities is not feasible, channel enhancement would be a more
509 feasible infrastructural solution. However, the impact of channel capacity increase on downstream
510 channels should be considered.

511 H&H models provide valuable insight for the determination of inundated areas and assessment of
512 damages. However, from the infrastructure management and hazard mitigation perspective, there is a
513 critical need for identifying the causes of such vulnerabilities in flood control network. In fact, the results
514 of the H&H models enable accurately determining the expected inundation maps and estimating flood
515 damages, which help preventing damages by avoiding further urban developments in areas with higher
516 risk of inundation and preparing emergency response needs for areas with high risk of inundation and
517 damage. However, from flood control infrastructure perspective, practitioners need to have a better
518 understanding regarding why a specific area has risk of inundation and how flood control network can be
519 improved in order to reduce the risk. The proposed framework enables vulnerability assessment and cause
520 identification and helps policy feasibility evaluation for risk reduction (e.g., development prioritization,
521 channels widening, storage facilities placement, storage capacity expansion, and redundancy building).
522 This all attributes to the proposed graph-based vulnerability index that encapsulates the impact of network
523 topology and storage facility on flood control network vulnerability. Hence, the proposed method and
524 measures can provide useful tools for decision-makers to effectively allocation limit resources to
525 infrastructure investments that systemically reduce vulnerability in different watersheds (or systems of
526 watersheds).

527 The proposed framework and this study present multiple avenues for further development in future
528 research. First, land characteristics such as the proportion of impervious surface, land slope, and
529 development pattern of each channel can be included in determining the overflow risk calculation. This
530 study aimed to assess the vulnerability for channels from a system-level perspective considering
531 topological network properties, and therefore, it does not consider any specific rainfall scenario for the
532 analysis. The outcomes of the H&H models can be integrated with the proposed vulnerability assessment
533 framework to examine the vulnerability in channels given different flooding scenarios (under different
534 rainfall intensities). In addition, a probabilistic scheme for considering flow change in each channel can
535 be included to encapsulate the flow dynamics of the flood control network. Moreover, future research can
536 consider the flow impact from hydrological factors, as well as the risk of overflow. For example, type of
537 the channel (i.e., meandering or straight) can greatly impacts the flow rate [56]. Hence, future research
538 can examine the impact of such factors on the vulnerability quantification. Finally, a system-level
539 vulnerability assessment can provide insight for decision makers to identify vulnerable components that
540 exacerbate the vulnerability of the whole system. However, prioritization of corresponding mitigation
541 actions requires a thorough understanding of the potential impacts (e.g., losses related to population,

542 environmental impacts) of different flood scenarios. Therefore, a combined system-level vulnerability
543 assessment and flood impact analysis will be conducted in our future research to enable the identification
544 of targeted mitigation actions based on their contribution to the reduction of flood impact.

545 **ACKNOWLEDGEMENT**

546 The authors would like to acknowledge the funding supports from the National Science Foundation
547 (award number: 1832662), Texas Sea Grant (under Grant Number NA18OAR4170088), National
548 Academies' Gulf Research Program Early-Career Research Fellowship (to Dr. Ali Mostafavi). Any
549 opinions, findings, and conclusions or recommendations expressed in this research are those of the
550 authors and do not necessarily reflect the views of the funding agencies.

551 **REFERENCES**

- 552 [1] Munich Re, Natural catastrophe losses at their highest for four years, Munich RE. (2017).
553 [https://www.munichre.com/en/media-relations/publications/press-releases/2017/2017-01-04-press-](https://www.munichre.com/en/media-relations/publications/press-releases/2017/2017-01-04-press-release/index.html)
554 [release/index.html](https://www.munichre.com/en/media-relations/publications/press-releases/2017/2017-01-04-press-release/index.html) (accessed July 29, 2019).
- 555 [2] S.N. Jonkman, Global perspectives on loss of human life caused by floods, *Nat. Hazards*. 34
556 (2005) 151–175. <https://doi.org/10.1007/s11069-004-8891-3>.
- 557 [3] S. Dong, A. Esmalian, H. Farahmand, A. Mostafavi, An integrated physical-social analysis of
558 disrupted access to critical facilities and community service-loss tolerance in urban flooding,
559 *Comput. Environ. Urban Syst.* 80 (2020) 101443.
560 <https://doi.org/10.1016/j.compenvurbsys.2019.101443>.
- 561 [4] J.C.J.H. Aerts, W.J. Botzen, K.C. Clarke, S.L. Cutter, J.W. Hall, B. Merz, E. Michel-Kerjan, J.
562 Mysiak, S. Surminski, H. Kunreuther, Integrating human behaviour dynamics into flood disaster
563 risk assessment /704/242 /706/689/2788 /706/2805 perspective, *Nat. Clim. Chang.* 8 (2018) 193–
564 199. <https://doi.org/10.1038/s41558-018-0085-1>.
- 565 [5] Y. Hirabayashi, R. Mahendran, S. Koirala, L. Konoshima, D. Yamazaki, S. Watanabe, H. Kim, S.
566 Kanae, Global flood risk under climate change, *Nat. Clim. Chang.* 3 (2013) 816–821.
567 <https://doi.org/10.1038/nclimate1911>.
- 568 [6] P. Milly, R. Wetherald, K. Dunne, T.D.- Nature, U. 2002, Increasing risk of great floods in a
569 changing climate, *Nature*. 415 (2002) 514–517. <https://doi.org/10.1038/415514a>.
- 570 [7] S. Mukherjee, S. Aadhar, D. Stone, V. Mishra, Increase in extreme precipitation events under
571 anthropogenic warming in India, *Weather Clim. Extrem.* 20 (2018) 45–53.
572 <https://doi.org/10.1016/j.wace.2018.03.005>.
- 573 [8] A. Ford, S. Barr, R. Dawson, J. Virgo, M. Batty, J. Hall, A multi-scale urban integrated
574 assessment framework for climate change studies: A flooding application, *Comput. Environ.*
575 *Urban Syst.* 75 (2019) 229–243. <https://doi.org/10.1016/j.compenvurbsys.2019.02.005>.
- 576 [9] M.C. Cunha, J.A. Zeferino, N.E. Simões, J.G. Saldarriaga, Optimal location and sizing of storage
577 units in a drainage system, *Environ. Model. Softw.* 83 (2016) 155–166.
578 <https://doi.org/10.1016/j.envsoft.2016.05.015>.
- 579 [10] E. Pérez-Molina, R. Sliuzas, J. Flacke, V. Jetten, Developing a cellular automata model of urban
580 growth to inform spatial policy for flood mitigation: A case study in Kampala, Uganda, *Comput.*
581 *Environ. Urban Syst.* 65 (2017) 53–65. <https://doi.org/10.1016/j.compenvurbsys.2017.04.013>.
- 582 [11] P. Berke, T. Larsen, C. Ruch, A computer system for hurricane hazard assessment, *Comput.*

- 583 Environ. Urban Syst. 9 (1984) 259–269. [https://doi.org/10.1016/0198-9715\(84\)90026-7](https://doi.org/10.1016/0198-9715(84)90026-7).
- 584 [12] W.J. Forsee, S. Ahmad, Evaluating urban storm-water infrastructure design in response to
585 projected climate change, *J. Hydrol. Eng.* 16 (2011) 865–873.
586 [https://doi.org/10.1061/\(ASCE\)HE.1943-5584.0000383](https://doi.org/10.1061/(ASCE)HE.1943-5584.0000383).
- 587 [13] R. Shariat, A. Roozbahani, A. Ebrahimian, Risk analysis of urban stormwater infrastructure
588 systems using fuzzy spatial multi-criteria decision making, *Sci. Total Environ.* 647 (2019) 1468–
589 1477. <https://doi.org/10.1016/j.scitotenv.2018.08.074>.
- 590 [14] S. Grimaldi, G.J.P. Schumann, A. Shokri, J.P. Walker, V.R.N. Pauwels, Challenges,
591 Opportunities, and Pitfalls for Global Coupled Hydrologic-Hydraulic Modeling of Floods, *Water
592 Resour. Res.* (2019). <https://doi.org/10.1029/2018WR024289>.
- 593 [15] A. Gori, R. Blessing, A. Juan, S. Brody, P. Bedient, Characterizing urbanization impacts on
594 floodplain through integrated land use, hydrologic, and hydraulic modeling, *J. Hydrol.* 568 (2019)
595 82–95. <https://doi.org/10.1016/j.jhydrol.2018.10.053>.
- 596 [16] T. Itoh, A. Ikeda, T. Nagayama, T. Mizuyama, Hydraulic model tests for propagation of flow and
597 sediment in floods due to breaking of a natural landslide dam during a mountainous torrent, *Int. J.
598 Sediment Res.* 33 (2018) 107–116. <https://doi.org/10.1016/j.ijsrc.2017.10.001>.
- 599 [17] V. Merwade, A. Cook, J. Coonrod, GIS techniques for creating river terrain models for
600 hydrodynamic modeling and flood inundation mapping, *Environ. Model. Softw.* 23 (2008) 1300–
601 1311. <https://doi.org/10.1016/j.envsoft.2008.03.005>.
- 602 [18] S.D. Brody, K.O. Atoba, Institutional Resilience, in: S. Fuchs, T. Thaler (Eds.), *Vulnerability
603 Resil. to Nat. Hazards*, Cambridge University Press, 2018: pp. 237–256.
604 <https://doi.org/10.1017/9781316651148>.
- 605 [19] Z.W. Kundzewicz, D.L.T. Hegger, P. Matczak, P.P.J. Driessen, Opinion: Flood-risk reduction:
606 Structural measures and diverse strategies, *Proc. Natl. Acad. Sci.* 115 (2018) 12321–12325.
607 <https://doi.org/10.1073/pnas.1818227115>.
- 608 [20] D.L.T. Hegger, P.P.J. Driessen, M. Wiering, H.F.M.W. Van Rijswick, Z.W. Kundzewicz, P.
609 Matczak, A. Crabbé, G.T. Raadgever, M.H.N. Bakker, S.J. Priest, C. Larrue, K. Ek, Toward more
610 flood resilience: Is a diversification of flood risk management strategies the way forward?, *Ecol.
611 Soc.* 21 (2016). <https://doi.org/10.5751/ES-08854-210452>.
- 612 [21] S.N. Mugume, D. Butler, Evaluation of functional resilience in urban drainage and flood
613 management systems using a global analysis approach, *Urban Water J.* 14 (2017) 727–736.
614 <https://doi.org/10.1080/1573062X.2016.1253754>.
- 615 [22] J.B. Ellis, Sustainable surface water management and green infrastructure in UK urban catchment
616 planning, *J. Environ. Plan. Manag.* 56 (2013) 24–41.
617 <https://doi.org/10.1080/09640568.2011.648752>.
- 618 [23] R.I. Ogie, S. Dunn, T. Holderness, E. Turpin, Assessing the vulnerability of pumping stations to
619 trash blockage in coastal mega-cities of developing nations, *Sustain. Cities Soc.* 28 (2017) 53–66.
620 <https://doi.org/10.1016/j.scs.2016.08.022>.
- 621 [24] R.I. Ogie, T. Holderness, S. Dunn, E. Turpin, Assessing the vulnerability of hydrological
622 infrastructure to flood damage in coastal cities of developing nations, *Comput. Environ. Urban
623 Syst.* 68 (2018) 97–109. <https://doi.org/10.1016/j.compenvurbsys.2017.11.004>.
- 624 [25] S.M. Rinaldi, J.P. Peerenboom, T.K. Kelly, Identifying, understanding, and analyzing critical

- 625 infrastructure interdependencies, *IEEE Control Syst. Mag.* (2001).
626 <https://doi.org/10.1109/37.969131>.
- 627 [26] S. Dong, T. Yu, H. Farahmand, A. Mostafavi, Bayesian modeling of flood control networks for
628 failure cascade characterization and vulnerability assessment, *Comput. Civ. Infrastruct. Eng.*
629 (2019) mice.12527. <https://doi.org/10.1111/mice.12527>.
- 630 [27] S. Dong, T. Yu, H. Farahmand, A. Mostafavi, Probabilistic modeling of cascading failure risk in
631 interdependent channel and road networks in urban flooding, *Sustain. Cities Soc.* 62 (2020)
632 102398. <https://doi.org/10.1016/j.scs.2020.102398>.
- 633 [28] S. Dong, T. Yu, H. Farahmand, A. Mostafavi, A Hybrid Deep Learning Model for Predictive
634 Flood Warning and Situation Awareness using Channel Network Sensors Data, (2020).
635 <http://arxiv.org/abs/2006.09201> (accessed August 15, 2020).
- 636 [29] W. Al-Sabhan, M. Mulligan, G.A. Blackburn, A real-time hydrological model for flood prediction
637 using GIS and the WWW, *Comput. Environ. Urban Syst.* 27 (2003) 9–32.
638 [https://doi.org/10.1016/S0198-9715\(01\)00010-2](https://doi.org/10.1016/S0198-9715(01)00010-2).
- 639 [30] H. Lü, T. Hou, R. Horton, Y. Zhu, X. Chen, Y. Jia, W. Wang, X. Fu, The streamflow estimation
640 using the Xinanjiang rainfall runoff model and dual state-parameter estimation method, *J. Hydrol.*
641 480 (2013) 102–114. <https://doi.org/10.1016/j.jhydrol.2012.12.011>.
- 642 [31] J.P. Amezquita-Sanchez, M. Valtierra-Rodriguez, H. Adeli, Current efforts for prediction and
643 assessment of natural disasters: Earthquakes, tsunamis, volcanic eruptions, hurricanes, tornados,
644 and floods (Invited Paper), *Sci. Iran.* 24 (2017) 2645–2664.
645 <https://doi.org/10.24200/sci.2017.4589>.
- 646 [32] A. Tejedor, A. Longjas, I. Zaliapin, E. Foufoula-Georgiou, Delta channel networks: 1. A graph-
647 theoretic approach for studying connectivity and steady state transport on deltaic surfaces, *Water*
648 *Resour. Res.* 51 (2015) 3998–4018.
649 [https://doi.org/10.1002/2014WR016577@10.1002/\(ISSN\)1944-7973.CONART1](https://doi.org/10.1002/2014WR016577@10.1002/(ISSN)1944-7973.CONART1).
- 650 [33] A. Tejedor, A. Longjas, D.A. Edmonds, I. Zaliapin, T.T. Georgiou, A. Rinaldo, E. Foufoula-
651 Georgiou, Entropy and optimality in river deltas, *Proc. Natl. Acad. Sci.* 114 (2017) 11651–11656.
652 <https://doi.org/10.1073/pnas.1708404114>.
- 653 [34] L. Lu, X. Wang, Y. Ouyang, J. Roningen, N. Myers, G. Calfas, Vulnerability of Interdependent
654 Urban Infrastructure Networks: Equilibrium after Failure Propagation and Cascading Impacts,
655 *Comput. Civ. Infrastruct. Eng.* 33 (2018) 300–315. <https://doi.org/10.1111/mice.12347>.
- 656 [35] V. Latora, M. Marchiori, Vulnerability and protection of infrastructure networks, *Phys. Rev. E -*
657 *Stat. Nonlinear, Soft Matter Phys.* 71 (2005). <https://doi.org/10.1103/PhysRevE.71.015103>.
- 658 [36] F. Maltinti, D. Melis, F. Annunziata, Road Network Vulnerability: A Review of the Literature, in:
659 2012. [https://doi.org/10.1061/41204\(426\)83](https://doi.org/10.1061/41204(426)83).
- 660 [37] E. Jenelius, L.G. Mattsson, Road network vulnerability analysis: Conceptualization,
661 implementation and application, *Comput. Environ. Urban Syst.* 49 (2015) 136–147.
662 <https://doi.org/10.1016/j.compenvurbsys.2014.02.003>.
- 663 [38] S. Dong, H. Wang, A. Mostafizi, X. Song, A network-of-networks percolation analysis of
664 cascading failures in spatially co-located road-sewer infrastructure networks, *Phys. A Stat. Mech.*
665 *Its Appl.* 538 (2020) 122971. <https://doi.org/10.1016/j.physa.2019.122971>.
- 666 [39] F. Meng, G. Fu, R. Farmani, C. Sweetapple, D. Butler, Topological attributes of network

- 667 resilience: A study in water distribution systems, *Water Res.* 143 (2018) 376–386.
668 <https://doi.org/10.1016/j.watres.2018.06.048>.
- 669 [40] P. Benjamin, L.G. Jonathan, N.H. Patrick, Applications of network analysis for adaptive
670 management of artificial drainage systems in landscapes vulnerable to sea level rise, *J. Hydrol.*
671 357 (2008). <https://doi.org/10.1016/j.jhydrol.2008.05.022>.
- 672 [41] R.I. Ogie, N. Shukla, F. Sedlar, T. Holderness, Optimal placement of water-level sensors to
673 facilitate data-driven management of hydrological infrastructure assets in coastal mega-cities of
674 developing nations, *Sustain. Cities Soc.* 35 (2017) 385–395.
675 <https://doi.org/10.1016/j.scs.2017.08.019>.
- 676 [42] Q.B. Travis, L.W. Mays, Optimizing retention basin networks, *J. Water Resour. Plan. Manag.* 134
677 (2008) 432–439. [https://doi.org/10.1061/\(ASCE\)0733-9496\(2008\)134:5\(432\)](https://doi.org/10.1061/(ASCE)0733-9496(2008)134:5(432)).
- 678 [43] E.H. Lee, Y.S. Lee, J.G. Joo, D. Jung, J.H. Kim, Investigating the impact of proactive pump
679 operation and capacity expansion on urban drainage system resilience, *J. Water Resour. Plan.*
680 *Manag.* 143 (2017). [https://doi.org/10.1061/\(ASCE\)WR.1943-5452.0000775](https://doi.org/10.1061/(ASCE)WR.1943-5452.0000775).
- 681 [44] A. Tejedor, A. Longjas, I. Zaliapin, E. Foufoula-Georgiou, Delta channel networks: 2. Metrics of
682 topologic and dynamic complexity for delta comparison, physical inference, and vulnerability
683 assessment, *Water Resour. Res.* 51 (2015) 4019–4045.
684 [https://doi.org/10.1002/2014WR016604@10.1002/\(ISSN\)1944-7973.CONART1](https://doi.org/10.1002/2014WR016604@10.1002/(ISSN)1944-7973.CONART1).
- 685 [45] R.I. Ogie, P. Perez, K.T. Win, K. Michael, Managing hydrological infrastructure assets for
686 improved flood control in coastal mega-cities of developing nations, *Urban Clim.* 24 (2018) 763–
687 777. <https://doi.org/10.1016/j.uclim.2017.09.002>.
- 688 [46] R. Ogie, T. Holderness, M. Dunbar, E. Turpin, Spatio-topological network analysis of
689 hydrological infrastructure as a decision support tool for flood mitigation in coastal mega-cities,
690 *Environ. Plan. B Urban Anal. City Sci.* 44 (2017) 718–739.
691 <https://doi.org/10.1177/0265813516637608>.
- 692 [47] Y. Wu, W. Xu, J. Fengt, S. Palaiiahnakote, T. Lu, Local and Global Bayesian Network based
693 Model for Flood Prediction, in: *Proc. - Int. Conf. Pattern Recognit.*, Institute of Electrical and
694 Electronics Engineers Inc., 2018: pp. 225–230. <https://doi.org/10.1109/ICPR.2018.8546257>.
- 695 [48] A.T. Murray, T.H. Grubestic, Overview of reliability and vulnerability in critical infrastructure, in:
696 *Adv. Spat. Sci.*, Springer International Publishing, 2007: pp. 1–8. https://doi.org/10.1007/978-3-540-68056-7_1.
- 698 [49] S. Wang, L. Hong, X. Chen, Vulnerability analysis of interdependent infrastructure systems: A
699 methodological framework, *Phys. A Stat. Mech. Its Appl.* 391 (2012) 3323–3335.
700 <https://doi.org/10.1016/j.physa.2011.12.043>.
- 701 [50] K. Rasoulkhani, A. Mostafavi, Resilience as an emergent property of human-infrastructure
702 dynamics: A multi-agent simulation model for characterizing regime shifts and tipping point
703 behaviors in infrastructure systems, *PLoS One.* 13 (2018).
704 <https://doi.org/10.1371/journal.pone.0207674>.
- 705 [51] M. Batouli, A. Mostafavi, Multiagent Simulation for Complex Adaptive Modeling of Road
706 Infrastructure Resilience to Sea-Level Rise, *Comput. Civ. Infrastruct. Eng.* 33 (2018) 393–410.
707 <https://doi.org/10.1111/mice.12348>.
- 708 [52] S.F. Balica, N.G. Wright, F. van der Meulen, A flood vulnerability index for coastal cities and its
709 use in assessing climate change impacts, *Nat. Hazards.* 64 (2012) 73–105.

- 710 <https://doi.org/10.1007/s11069-012-0234-1>.
- 711 [53] D. Koller, N. Friedman, Probabilistic graphical models: principles and techniques, 2009.
712 [https://books.google.com/books?hl=en&lr=&id=7dzpHCHzNQ4C&oi=fnd&pg=PR9&dq=probabi](https://books.google.com/books?hl=en&lr=&id=7dzpHCHzNQ4C&oi=fnd&pg=PR9&dq=probabilistic+graphical+models&ots=pw5AAj0YyK&sig=IAQL0tp1eVX4N4MQFCvP4i82jpc)
713 [listic+graphical+models&ots=pw5AAj0YyK&sig=IAQL0tp1eVX4N4MQFCvP4i82jpc](https://books.google.com/books?hl=en&lr=&id=7dzpHCHzNQ4C&oi=fnd&pg=PR9&dq=probabilistic+graphical+models&ots=pw5AAj0YyK&sig=IAQL0tp1eVX4N4MQFCvP4i82jpc) (accessed
714 October 16, 2019).
- 715 [54] Y.K. Tung, Risk-based analysis of a detention basin for urban runoff control, *J. Appl. Water Eng.*
716 *Res.* 6 (2018) 200–209. <https://doi.org/10.1080/23249676.2017.1287019>.
- 717 [55] S.F. Balica, N.G. Wright, F. van der Meulen, A flood vulnerability index for coastal cities and its
718 use in assessing climate change impacts, *Nat. Hazards.* 64 (2012) 73–105.
719 <https://doi.org/10.1007/s11069-012-0234-1>.
- 720 [56] C. of Houston, Harris County Flood Control District, (2017) 1–15. <https://www.hcfc.org/>
721 (accessed December 7, 2019).
- 722 [57] Project Brays, (n.d.). <https://www.projectbrays.org/about-project-brays/> (accessed December 7,
723 2019).
- 724 [58] M. Shams, G. Ahmadi, D.H. Smith, Computational modeling of flow and sediment transport and
725 deposition in meandering rivers, *Adv. Water Resour.* 25 (2002) 689–699.
726 [https://doi.org/10.1016/S0309-1708\(02\)00034-9](https://doi.org/10.1016/S0309-1708(02)00034-9).
- 727